

# Analysis of Cross-layer Interaction in Multi-rate 802.11 WLANs

Jaehyuk Choi, Kihong Park, *Member, IEEE*, and Chong-kwon Kim, *Member, IEEE*

## Abstract

Recent works in empirical 802.11 wireless LAN performance evaluation have shown that cross-layer interactions in WLANs can be subtle, sometimes leading to unexpected results. Two such instances are: (i) significant throughput degradation resulting from automatic rate fallback (ARF) having difficulty distinguishing collision from channel noise, and (ii) scalable TCP over DCF performance that is able to mitigate the negative performance effect of ARF by curbing multiple access contention even when the number of stations is large. In this paper, we present a framework for analyzing complex cross-layer interactions in 802.11 WLANs, with the aim of providing effective tools for understanding and improving WLAN performance. We focus on cross-layer interactions between ARF, DCF, and TCP, where ARF adjusts coding at the physical layer, DCF mediates link layer multiple access control, and TCP performs end-to-end transport. We advance station-centric Markov chain models of ARF, ARF-DCF with and without RTS/CTS, and TCP over DCF that may be viewed as multi-protocol extensions of Bianchi's IEEE 802.11 model. We show that despite significant increase in complexity the analysis framework leads to tractable and accurate performance predictions. Our results complement empirical and simulation-based findings, demonstrating the versatility and efficacy of station-centric Markov chain analysis for capturing cross-layer WLAN dynamics.

## I. INTRODUCTION

### A. Background

IEEE 802.11 wireless LANs (WLANs) have become the predominant wireless Internet access technology. In addition to realizing a specific form of CSMA/CA, they implement several performance

J. Choi and C. Kim are with the School of Computer Science and Engineering, Seoul National University, Seoul, 151-744 Korea, e-mail: {jhchoi, ckim}@popeye.snu.ac.kr.

K. Park is with the Dept. of Computer Science, Purdue University, IN 47907, U.S.A, e-mail: park@cs.purdue.edu.

A preliminary version of this paper appeared in the proceedings of the IEEE INFOCOM 2007 conference [8].

enhancement features including support for multi-rate coding at the physical layer. Rate adaptation uses 802.11's multiple code rates to respond to the variability of a wireless channel by selecting the data rate at which a frame is encoded. Distributed coordination function (DCF) arbitrates medium access among wireless clients using CSMA with binary exponential backoff, determining when a frame transmission is attempted. TCP, which transports the bulk of Internet traffic, influences the traffic impinging on DCF and ARF. DCF and ARF, in turn, help shape the end-to-end network characteristics experienced by TCP. All three protocols employ feedback control. Understanding their cross-layer interactions is the focus of this paper.

Our starting point is the analysis of rate adaptation. When the signal-to-noise ratio (SNR) is determined to be low, rate adaptation selects a low data rate which yields greater resilience to noise. A widely deployed method is automatic rate fallback (ARF) [16] which uses up/down thresholds to select a data rate. In ARF two consecutive transmission failures—i.e., 802.11 acknowledgement (ACK) frames are not received—result in rate downshift to the next lower rate. After ten consecutive frame transmission successes, the next higher rate is selected for transmission of the next data frame. If delivery of the eleventh frame transmitted at a higher rate is unsuccessful, ARF triggers immediate fallback to the previously used data rate. Most rate adaptation implementations are variants of the canonical ARF based on an up/down counter mechanism [3], [17], [20]. In some cases, statistics of previous frame deliveries from 802.11 ACK feedback are used in rate adaptation [6], [27].

Although well-intentioned, the design of ARF does not consider cross-layer dependencies that can significantly impact performance. ARF assumes that all transmission failures are due to channel errors ignoring that failures can result from collisions. As a result ARF may respond to frame collisions which cannot be distinguished from channel errors based on missing 802.11 ACKs alone, resulting in unnecessary rate downshift even when channel noise is low. Empirical 802.11b WLAN measurements [9] have shown that under moderate multiple access contention (4–15 wireless stations) WLAN throughput declines drastically, not because of network congestion but ARF confusing collision with channel noise. In the same physical environment, fixing the data rate at 11 Mbps (by default, ARF is enabled in WLAN cards) can give a 5-fold increase in system throughput. In [9] it is also shown that when TCP is active over ARF and DCF (the typical modus operandi for wireless Internet access), the detrimental influence of ARF is largely mitigated. Using experiments and simulation it is shown that TCP over DCF curtails effective multiple access contention which desensitizes ARF against misleading collision cues. The collective dynamics of ARF, DCF, and TCP can be subtle and complex.

### B. New Contribution

Modeling cross-layer protocol interactions, in general, is a challenging task. Modeling the collective behavior of ARF, DCF, and TCP is no exception. In this paper, we tackle the problem of capturing cross-layer protocol interactions in 802.11 WLANs, with the aim of providing effective analysis tools for understanding and improving WLAN performance. First, we consider MAC layer interactions between ARF and DCF's exponential backoff which are joined by frame transmission events at the multi-rate PHY layer. We define an ARF Markov chain generated by the point process of transmission events. We derive a closed-form solution parameterized by the up/down thresholds and rate-dependent transmission failure probabilities which gives the probability of choosing a specific data rate in steady-state. Although the ARF chain is significantly different from Bianchi's DCF chain [5], symmetries in the ARF chain admit derivation of closed-form expressions relating the key variables. To the best of our knowledge, this is the first Markov chain model of ARF. The ARF chain is joined with a multi-rate extension of Bianchi's DCF chain [5] parameterized by ARF's rate probabilities which gives the rate-dependent transmission failure and attempt probabilities. The state-space explosion problem of the combined ARF-DCF system is handled by finding a globally consistent solution to the two parameterized subsystems—afforded by modular coupling—that lends itself to fixed-point methods. We validate the analysis by comparing the predicted results with *ns-2* simulations which show the qualitative fidelity and quantitative accuracy of the joint ARF-DCF model. We show that the impact of RTS/CTS is easily incorporated in this framework.

Second, we incorporate the influence of TCP running over IEEE 802.11 infrastructure WLANs with ARF. Several solutions have been proposed for improving ARF performance [7], [17], [23] but the problem is more entangled because WLAN performance is influenced by cross-layer interactions with TCP. Since the bulk of Internet traffic is transported by TCP, capturing interaction between DCF, ARF, and TCP is relevant for understanding WLAN based Internet access performance. The empirical findings in [9] show that TCP-over-DCF is able to throttle multiple access contention in a WLAN, even when the number of contending stations is large, such that ARF's miscues from frame collision and consequent throughput degradation is mitigated. Essential to this is the scalable throughput of TCP-over-DCF which drastically reduces the frequency of consecutive frame collisions. As in the ARF-DCF model, we adopt a station-centric approach where TCP-over-DCF dynamics is captured by a Markov chain over a station's backlog state, incorporating the symmetry of multiple access contention introduced by DCF. We show that the combined model yields accurate predictions of both coarse-granular (throughput) and fine-granular (station dynamics) TCP-over-WLAN performance.

*Remark.* Our cross-layer WLAN models may be viewed as advancing the station-centric Markov chain analysis approach followed by Bianchi [5] whose surprisingly accurate performance predictions are only now being better understood [24]. Our results show that modular station-centric Markov modeling—even when the underlying Markov chains for ARF, DCF, and TCP are very different—can accurately capture WLAN performance in the presence of cross-layer interactions.

### C. Related Work

There have been a large number of studies on the performance of IEEE 802.11 DCF. Bianchi’s Markov chain model of IEEE 802.11 DCF [5] has been extended in several directions including explicit consideration of carrier sense [33], maximum retransmission count [28], prioritized channel access [29], and capture effect [10]. They represent direct extensions of the DCF chain. A multi-rate generalization of Bianchi’s model has been considered in [32], albeit with the severe restriction that stations are assigned fixed data rates. An interesting technical advance is a Markov chain model over the state-space counting the number of stations in a backoff stage [24] that trades Bianchi’s independence assumption with stochastic approximation using average (i.e., deterministic) dynamics. The results are relevant because they help explain why the independence assumption leads to accurate quantitative predictions, a hallmark of Bianchi’s Markov chain model.

Empirical performance evaluation of ARF on 802.11b WLANs performance were provided in [9], which showed drastic throughput degradation caused by ARF under moderate multiple access contention. ARF’s unintended side effect has been a source of confusion in both academia and industry. For example, in [26] sharp WLAN throughput decline in an experimental WLAN was attributed to CSMA’s multiple access contention. In [15] it is noted that “as the number of contending stations increases, aggregate capacity drops precipitously (to less than 1 Mb/s with 10 contending stations)” which is attributed to CSMA. With ARF disabled, empirical findings in [9] show that WLAN throughput decreases gradually with increasing contention level. TCP-over-WLAN performance has been considered generally poor due to channel noise and multiple access contention [22], [31], given TCP’s sensitive dependence on packet loss rate ( $\propto p^{-1/2}$ ) [19]. This has prompted solutions aimed at reducing TCP’s exposure to frame errors and collisions on the wireless channel [4], [11], [30]. In [9] it is shown through experiment and simulation that TCP-over-WLAN achieves high throughput, even when the number of contending stations is large. Our analysis provides an explanation for the surprisingly agile TCP-over-WLAN performance.

Several methods have been proposed to deal with ARF’s noise vs. collision differentiation problem [7], [17], [18], [20], [23]. These results focus on improving ARF performance through enhanced algorithms

and protocol mechanisms. For example, in [17] a modified ARF that makes use of RTS/CTS is proposed which exploits the fact that RTS frames are small and always encoded at the lowest data rate. Therefore a RTS frame transmission failure is likely the result of collision, whereas data frame transmission failures following a successful RTS/CTS handshake are likely due to channel error. An overview of existing methods can be found in [12].

## II. ANALYTICAL MODEL OF ARF

In this section, we present a station-centric Markov chain model of ARF, its closed-form solution, and performance validation.

### A. Markov Chain Model of ARF

We consider a multi-rate IEEE 802.11 WLAN with  $L$  different data rates, denoted by  $R_1 < R_2 < \dots < R_L$  in units of Mbps, where the WLAN consists of  $N$  homogeneous stations subject to the same channel conditions in steady-state. For example, in 802.11b  $L = 4$  with rates 1, 2, 5.5, and 11 Mbps. In 802.11a/g  $L = 8$  with data rates 6, 9, 12, 18, 24, 36, 48, 54 Mbps. For each rate  $R_i$  and given a fixed frame size, each station is assumed to have a frame error rate (FER)  $e_i$  obeying  $e_1 \leq e_2 \leq \dots \leq e_i \leq \dots \leq e_L$  due to the increased robustness of 802.11 PHY modulation at lower data rates. We ignore the effect of correlated frame errors that may stem from fading channels. Following Bianchi [5], we introduce the independence assumption that in equilibrium a frame transmission experiences collision with constant and independent probability  $p$ . Then, the conditional frame failure probability (from collision or noise) of a frame transmitted at rate  $R_i$  is given by  $p_i = 1 - (1 - p)(1 - e_i)$ , where  $0 < p_i < 1$ .

Let  $\theta_d$  and  $\theta_u$  denote the up and down thresholds of ARF, respectively, where  $\theta_d$  consecutive transmission failures result in a rate downshift and  $\theta_u$  consecutive successes trigger a rate upshift (more precisely, probing to higher rate, i.e., if the first transmission attempt fails after a rate upshift, it immediately falls back to the previously used lower rate). For example, in the Enterasys RoamAbout 802.11 DS High Rate card [3] (similarly for Cisco Aironet 350 cards), downshifting is triggered by  $\theta_d = 2$  consecutive failures to receive an 802.11 ACK frame. The up-threshold is  $\theta_u = 10$ . A key weakness of current implementations of ARF is that channel noise and collision are not effectively distinguished. This can result in significant throughput degradation (a bell-shaped throughput curve) stemming from multiple access contention [9].

Our aim in this section is to capture the workings and impact of ARF on WLAN performance. Bianchi's DCF Markov chain [5] models the exponential backoff process by considering a Markov chain induced

by the backoff stage and time counter. The chain is driven by the point process of frame transmission events under the aforementioned independence assumption. We define a Markov chain generated by the same point process that tracks the data rate selected by ARF. Let  $r(t) \in \{1, 2, \dots, L\}$  denote the data rate index. Let  $c(t)$  ( $-\theta_d + 1 \leq c(t) \leq \theta_u - 1$ ) denote the counter of consecutive failures ( $c(t) < 0$ ) or successes ( $c(t) > 0$ ) at rate  $r(t)$ . We adopt a discrete-time model indexed by  $t$  which corresponds to the end time of the  $t$ -th transmission event of a tagged station. Assuming  $e_1, \dots, e_L$  and  $p$  are given—how  $p$  is determined is addressed in Section III—the ARF Markov chain  $(r(t), c(t))$  is depicted in Fig. 1. The chain captures the rate-shift behavior of ARF including the up-rate probing mechanism. Note that we reduced the number of states to a minimum by integrating all the identical states into a state. For example, the boundary states in rate-downshift (i.e. states whose  $r(t) = 1$  and  $c(t) < 0$ ) can be incorporated into a state  $(1, -1)$ . For  $p_i$  ( $0 < p_i < 1$ ), the chain is irreducible and aperiodic, and we are interested in finding

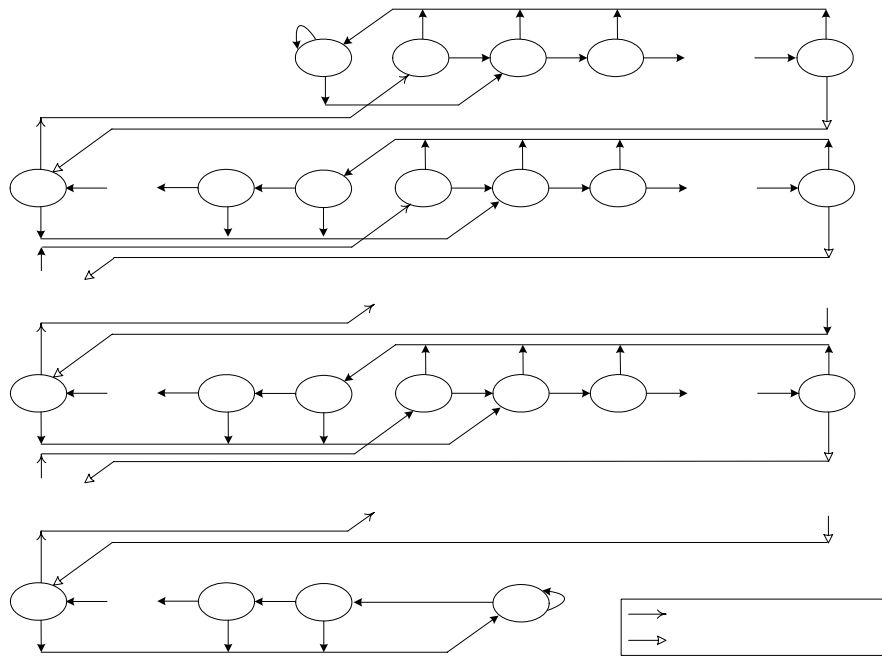


Fig. 1. Markov chain model of ARF with  $L$  data rates, up-threshold  $\theta_u$  and down-threshold  $\theta_d$  where  $u = \theta_u - 1$  and  $d = \theta_d - 1$ .

the unique equilibrium probability

$$\Pi_i = \sum_{k=-\theta_d+1}^{\theta_u-1} r_{i,k}, \quad 1 \leq i \leq L,$$

where  $r_{i,k} = \lim_{t \rightarrow \infty} P\{r(t) = i, c(t) = k\}$ .  $\Pi_i$  captures a station's probability of transmitting at data rate

$R_i$ . Different rate adaptation methods result in different  $\Pi_i$  which provides a well-defined interface for integrating with DCF. Our modular cross-layer WLAN analysis approach is not limited to ARF, although one of the technical contributions of this paper is providing a rigorous performance analysis of ARF.

### B. Steady-state Solution of ARF Markov Chain

Although different in structure from Bianchi's DCF chain [5], the ARF Markov chain possesses regularities that admit to a closed-form solution for  $\Pi_i$  as a function of the system parameters  $p_i$ ,  $\theta_d$  and  $\theta_u$ . A key observation to finding the solution is that *the ARF chain can be transformed into a coarsified birth-death chain* by aggregating the states corresponding to  $r_{i,k}$  for different counter values  $k$  into a single macro state. This is depicted in Fig. 2. Since the equilibrium distribution of a  $L$ -state

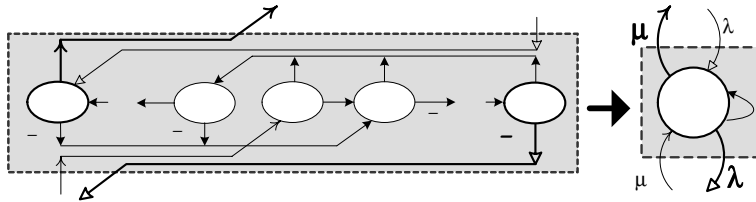


Fig. 2. Dimension reduction: ARF Markov chain aggregation into coarsified birth-death chain.

discrete-time birth-death chain with birth probabilities  $\lambda_i$  ( $i \in \{1, 2, \dots, L-1\}$ ) and death probabilities  $\mu_i$  ( $i \in \{2, \dots, L\}$ ) is given by

$$\Pi_1 = \frac{1}{1 + \sum_{j=1}^{L-1} (\prod_{k=1}^j \frac{\lambda_k}{\mu_{k+1}})} \text{ and } \Pi_i = \frac{\lambda_{i-1}}{\mu_i} \Pi_{i-1}, \quad (1)$$

for  $i \in \{2, \dots, L\}$ , it suffices to find closed-form solutions for  $\lambda_i$  and  $\mu_i$  in terms of  $p_i$ ,  $\theta_d$  and  $\theta_u$ . In the following, we set  $u = \theta_u - 1$  and  $d = \theta_d - 1$  for notational simplicity.

$\lambda_i$  and  $\mu_i$  denote the state transition probabilities of increasing the current rate  $i$  to  $i+1$  and decreasing the current rate  $i$  to  $i-1$ , respectively. They can be written as

$$\lambda_i = \frac{r_{i,u} P\{i+1, -d | i, u\}}{P\{\text{current rate} = R_i\}} = \frac{r_{i,u}}{\Pi_i} (1 - p_i), \quad (2)$$

$$\mu_i = \frac{r_{i,-d} P\{i-1, 0 | i, -d\}}{P\{\text{current rate} = R_i\}} = \frac{r_{i,-d}}{\Pi_i} p_i. \quad (3)$$

Note that for  $\lambda_i$  the index is defined for  $i \in \{1, \dots, L-1\}$  whereas for  $\mu_i$  the index ranges over  $i \in \{2, \dots, L\}$ . The ARF Markov chain (Fig. 1) obeys the balance equations

$$r_{i,k} = (1 - p_i) r_{i,k-1}, \quad 1 \leq i < L, \quad 2 \leq k \leq u, \quad (4)$$

$$r_{i,k} = p_i r_{i,k+1}, \quad 1 < i \leq L, \quad -d < k \leq -2, \quad (5)$$

which yield

$$r_{i,k} = (1 - p_i)^{k-1} r_{i,1}, \quad 1 \leq i < L, \quad 1 \leq k \leq u, \quad (6)$$

$$r_{i,k} = p_i^{-(k+1)} r_{i,-1}, \quad 1 < i \leq L, \quad -d < k \leq -1. \quad (7)$$

We also get the balance equations

$$r_{i,1} = (1 - p_i) \sum_{k=-d}^0 r_{i,k}, \quad 1 \leq i < L, \quad (8)$$

$$r_{L,1} = (1 - p_L) \sum_{k=-d}^{-1} r_{L,k}, \quad (9)$$

$$r_{i,-1} = p_i \sum_{k=0}^u r_{i,k} \quad 1 \leq i \leq L, \quad (10)$$

$$r_{i,0} = p_{i+1} r_{i+1,-d}, \quad 1 \leq i < L, \quad (11)$$

$$r_{i,-d} = p_i r_{i,-d+1} + (1 - p_{i-1}) r_{i-1,u}, \quad 1 < i \leq L. \quad (12)$$

*Step 1:* First, we consider  $\lambda_i$ .  $\Pi_i$  can be split into two parts

$$\Pi_i = \sum_{k=-d}^u r_{i,k} = \sum_{k=-d}^0 r_{i,k} + \sum_{k=1}^u r_{i,k}.$$

Using Eqs. (8) and (6), we obtain

$$\begin{aligned} \Pi_i &= \frac{r_{i,1}}{1 - p_i} + r_{i,1} \sum_{k=1}^u (1 - p_i)^{k-1} \\ &= \frac{1 - (1 - p_i)^{u+1}}{p_i(1 - p_i)} r_{i,1} = \frac{1 - (1 - p_i)^{u+1}}{p_i(1 - p_i)^u} r_{i,u}. \end{aligned} \quad (13)$$

Applying Eq. (13) to Eq. (2),

$$\lambda_i = \frac{r_{i,u}}{\Pi_i} (1 - p_i) = \frac{p_i(1 - p_i)^{u+1}}{1 - (1 - p_i)^{u+1}} = \frac{p_i(1 - p_i)^{\theta_u}}{1 - (1 - p_i)^{\theta_u}}. \quad (14)$$

*Step 2:* Next, we consider  $\mu_i$ .  $\Pi_i$  may also be written as

$$\Pi_i = \sum_{k=-d}^u r_{i,k} = r_{i,-d} + \sum_{k=-d+1}^{-1} r_{i,k} + \sum_{k=0}^u r_{i,k}.$$

Using Eqs. (7), (10) and (5), we get

$$\begin{aligned} \Pi_i &= r_{i,-d} + \frac{1 - p_i^{d-1}}{1 - p_i} r_{i,-1} + \frac{r_{i,-1}}{p_i} \\ &= r_{i,-d} + \frac{1 - p_i^d}{(1 - p_i)p_i} r_{i,-1} = r_{i,-d} + \frac{1 - p_i^d}{(1 - p_i)p_i^{d-1}} r_{i,-d+1}. \end{aligned} \quad (15)$$

From the definition of  $\lambda_i$ ,  $(1-p_{i-1})r_{i-1,u} = \lambda_{i-1}\Pi_{i-1}$ . The detailed balance equation,  $\lambda_{i-1}\Pi_{i-1} = \mu_i\Pi_i$ , holds for the birth-death chain. Applying these to Eq. (12), we have

$$r_{i,-d} = p_i r_{i,-d+1} + \mu_i \Pi_i = p_i r_{i,-d+1} + p_i r_{i,-d}$$

which yields

$$r_{i,-d+1} = \frac{1-p_i}{p_i} r_{i,-d}. \quad (16)$$

Substituting Eq. (16) into Eq. (15), we get

$$\Pi_i = r_{i,-d} + \frac{1-p_i^d}{(1-p_i)p_i^{d-1}} \frac{1-p_i}{p_i} r_{i,-d} = \frac{1}{p_i^d} r_{i,-d}.$$

Finally, we obtain the departure rate

$$\mu_i = \frac{r_{i,-d}}{\Pi_i} p_i = p_i^{d+1} = p_i^{\theta_d}. \quad (17)$$

Substituting  $\lambda_i$  and  $\mu_i$  into Eq. (1), we arrive at an expression for  $\Pi_i$  as a function of  $p_k$  ( $k = 1, \dots, L$ ),  $\theta_u$  and  $\theta_d$ .

### C. ARF Performance Validation

We evaluate the accuracy of the ARF model by comparing the analytical results with those of *ns-2* simulations with CMU's wireless extension. We simulated an IEEE 802.11b WLAN in the saturated

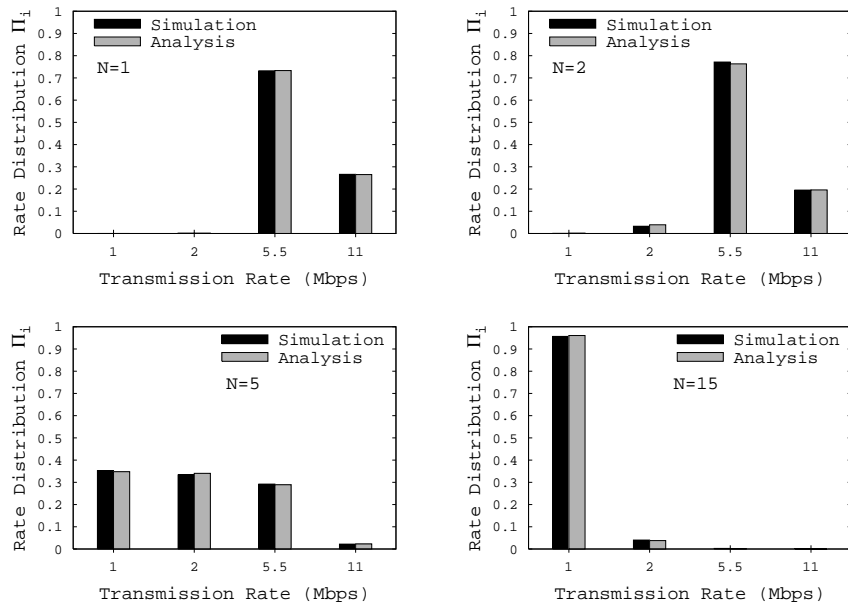


Fig. 3. Rate distribution ( $\Pi_i$ ): Analysis vs. simulation ( $\theta_u = 10$ ,  $\theta_d = 2$ ) for  $N = 1, 2, 5$ , and 15 stations in IEEE 802.11b.

throughput regime (i.e., all stations are infinite source) where  $L = 4$  with data rates 1, 2, 5.5, and 11 Mbps. The ARF thresholds are  $\theta_u=10$  and  $\theta_d=2$ , and payload size is 1000 bytes. Channel conditions were set to generate frame error rates (FERs) based on empirical PHY measurements [2].  $p_i$  is set to the value observed in the simulations. The case where  $p_i$  is predicted as part of the analysis is treated in the next section.

Fig. 3 compares the steady-state rate distribution probability  $\Pi_i$  obtained from the ARF Markov chain model and  $ns-2$  simulations. Irrespective of the number of stations  $N = 1, 2, 10,$  and  $25$ , we find a close match between the analytical results and simulation. In addition to quantitative accuracy, the ARF model predicts the qualitative trend of current ARF implementations that dwell most of the time at low data rates even for moderate contention levels [9].

Fig. 4 shows the comparison between analysis and simulation for a 802.11g WLAN with  $L = 8$  data rates 6, 9, 12, 18, 24, 36, 48, 54 Mbps. For small  $N$  where collision rates are low, ARF responds to channel noise and system throughput remains high. At  $N = 10$ , the weakness of ARF manifests starkly where stations predominantly use the lowest data rate 6 Mbps despite the fact that increased frame transmission failures are due to collision, not channel noise.

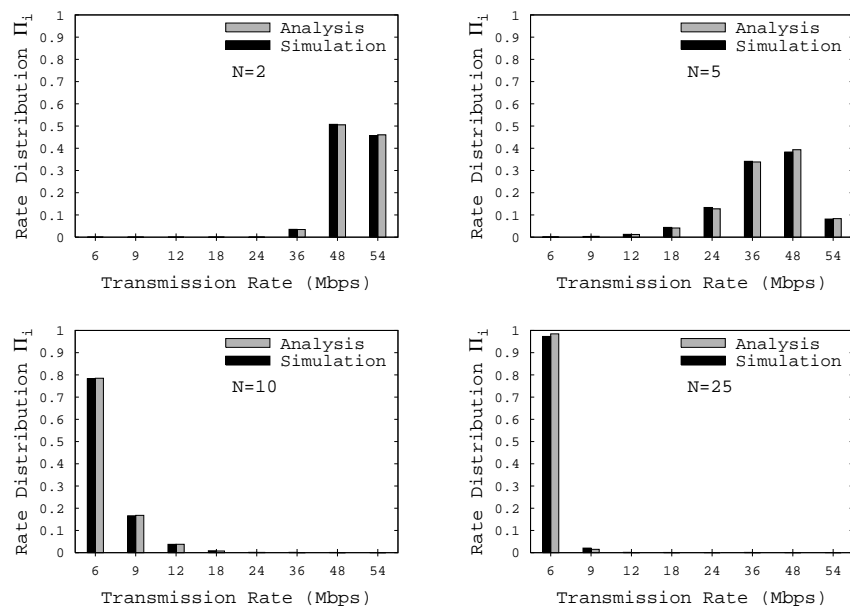


Fig. 4. Rate distribution ( $\Pi_i$ ): Analysis vs. simulation ( $\theta_u = 10, \theta_d = 2$ ) for  $N = 2, 5, 10,$  and  $25$  in IEEE 802.11g.

### III. PERFORMANCE ANALYSIS OF COMBINED ARF-DCF

The previous section modeled the behavior of ARF assuming  $p_1, \dots, p_L$  are given. In this section, we tackle the problem of analyzing multi-rate IEEE 802.11 WLANs with DCF and ARF when their influence extends in both directions.

#### A. Integrated ARF-DCF Multi-rate Model

We consider a multi-rate IEEE 802.11 WLAN with  $L$  data rates  $R_1 < R_2 < \dots < R_L$  accessed by  $N$  stations. Bianchi's DCF Markov chain  $(s(t), b(t))$  is driven by the point process of frame transmission events under the independence assumption that a frame experiences the same channel condition in equilibrium [5].  $s(t)$  and  $b(t)$  denote the backoff stage and backoff time counter, respectively. Our ARF chain  $(r(t), c(t))$  is generated by the same point process which determines what data rate is used at backoff stage  $s(t)$  when  $b(t) = 0$ . The outcome of the transmission attempt prescribes the next state. The combined system  $(s(t), b(t), r(t), c(t))$  can be modeled as a Markov chain over their product space where the frame transmission failure probability  $p_i$  depends on the current rate  $r(t) = i$ . Not all state combinations, however, are reachable. For example, starting from initial state  $s(0) = b(0) = 0$ ,  $r(0) = L$  and  $c(0) = 1$ , the system cannot reach  $(x, y, L, z)$  for  $x > \theta_d$  due to the rate downshift operation of ARF. Thus  $\theta_d$  determines the state-space boundary that envelops the irreducible core. The latter is also aperiodic, hence ergodic.

#### B. Fixed-point Solution under Modular Coupling

A static multi-rate 802.11 model without rate adaptation is considered in [32] where each station in group  $i$  is assumed to use a *fixed* rate  $R_i$ , partitioned into  $L$  groups  $n_1 + \dots + n_L = N$ . Consequently,  $n_i$  is fixed as well. Under the independence assumption, a station in group  $i \in \{1, \dots, L\}$  obeys Bianchi's DCF chain with homogenous transition rate  $p_i$ . Since frame collisions are assumed to occur independently—different rates only lead to variable collision slot durations—Bianchi's frame transmission attempt rate

$$\tau_i = \frac{2(1 - 2p_i)}{(1 - 2p_i)(W_0 + 1) + p_i W_0 (1 - (2p_i)^m)} \quad (18)$$

holds with the added dependence on  $i \in \{1, \dots, L\}$ . Here  $m$  is the maximum backoff stage and  $W_0$  is the minimum backoff window size. When ARF is present, a station will adjust its data rate over time as frame transmissions succeed or fail. This implies that  $n_1, \dots, n_L$  are not given but *determined* by the dynamics of the integrated multi-rate WLAN with ARF and DCF. That is,  $n_i(t)$  is a function of time.

The state-space explosion problem makes direct analysis difficult. We approximate the steady-state solution of the combined ARF-DCF Markov chain using *modular coupling*. First, we find parameterized solutions of the ARF chain  $(r(t), c(t))$  and DCF chain  $(s(t), b(t))$  separately, then resolve the parameters to find a globally consistent solution for the combined system. In the ARF chain, the closed-form solution (cf. Section II) has the form

$$\Pi_i = f(p_1, \dots, p_L, \theta_d, \theta_u), \quad i \in \{1, \dots, L\}, \quad (19)$$

parameterized by  $p_i$  which is determined by the DCF chain. In the DCF chain, a solution for  $(p_i, \tau_i)$  is sought that satisfies Eq. (18) and

$$p_i = 1 - (1 - \bar{\tau})^{N-1}(1 - e_i) \quad (20)$$

where  $\bar{\tau} = \sum_{i=1}^L \Pi_i \tau_i$  is the mean transmission rate of a station (i.e., averaged over the  $L$  data rates that it may employ). The latter is the fixed-point formulation of Bianchi's DCF Markov chain.

In the combined ARF-DCF model, we make use of the fact that Eq. (20) is parameterized by  $\Pi_i$ ,  $i \in \{1, \dots, L\}$ , since  $\sum_{i=1}^L \Pi_i (1 - \tau_i) = (1 - \bar{\tau})$  represents the probability that a station does not transmit in a random slot.  $\Pi_i$ , in turn, is determined by the ARF chain. We arrive at a globally consistent solution by finding  $(p_i, \tau_i, \Pi_i)$ ,  $i \in \{1, \dots, L\}$ , that satisfy Eqs. (18), (20), and (19) using fixed-point techniques. Thus the combined ARF-DCF model can be viewed as a multi-protocol extension of Bianchi's model whose total dimension has increased by one from  $(p_i, \tau_i)$  to  $(p_i, \tau_i, \Pi_i)$ .

### C. Combined ARF-DCF Throughput Computation

With  $(p_i, \tau_i, \Pi_i)$  at hand, the main issue involved in computing the combined ARF-DCF throughput is estimating the slot duration when frames collide.  $\Pi_i$  plays an important role in this regard. Let  $P_{S(i)}$  ( $i = 1, 2, \dots, L$ ) denote the probability that a successful transmission at rate  $i$  occurs at a slot in steady-state. We have  $P_{S(i)} = N \Pi_i \tau_i (1 - \bar{\tau})^{N-1} (1 - e_i)$ . The probability that a frame transmitted at rate  $i$  does not collide but experiences a frame error is  $P_{Err(i)} = N \Pi_i \tau_i (1 - \bar{\tau})^{N-1} e_i$ . The probability that a slot is idle is given by  $P_I = (1 - \bar{\tau})^N$ . Hence the probability that a frame transmission collides is

$$P_C = 1 - P_I - \sum_{i=1}^L P_{S(i)} - \sum_{i=1}^L P_{Err(i)}.$$

The normalized system throughput contributed by frames transmitted at rate  $i$  is given by

$$X_i = \frac{P_{S(i)} S_i}{P_I \sigma + T_S + T_{Err} + T_C} \quad (21)$$

where  $S_l$  is the payload size,  $\sigma$  is the slot time,  $T_S$ ,  $T_{Err}$ , and  $T_C$  are the average durations of successful, erroneous, and collided transmissions, respectively. Let  $X = \sum_{i=1}^L X_i$  denote aggregate throughput.  $T_S$  and  $T_{Err}$  are given by

$$T_S = \sum_{k=1}^L P_{S(k)} T_{S(k)}, \quad T_{Err} = \sum_{k=1}^L P_{Err(k)} T_{Err(k)},$$

where for the basic access method in DCF (i.e., RTS/CTS is disabled) we have

$$T_{S(k)} = T_{PHY} + (S_h + S_l) / R_k + \text{SIFS} + \text{ACK} + \text{DIFS},$$

$$T_{Err(k)} = T_{PHY} + (S_h + S_l) / R_k + \text{EIFS}.$$

$T_{PHY}$  is the duration of a PHY header and  $S_h$  represents the length of a MAC header. What remains is to estimate  $T_C$ .

A distinctive feature of multi-rate frame collision is that *the collision time is determined by a frame encoded with the lowest data rate* which has the longest transmission time [5],[32]. Collisions involving multiple stations can be approximated by pairwise collisions [5] as they dominate the higher order terms. In a multi-rate system, an additional source of combinatorial explosion arises due to the different ways  $N$  stations using data rates  $R_1, \dots, R_L$  can collide. Let  $(n_1, \dots, n_L)$  denote the average number of stations using rates  $R_1, \dots, R_L$  in steady-state. The number of combinations to consider is  $(N + L - 1)! / N!(L - 1)!$  which is too unwieldy. We employ a ‘‘mean field’’ approximation as follows.  $T_C$  is bounded by

$$P_C \left( T_{PHY} + \frac{S_h + S_l}{R_L} + \text{EIFS} \right) < T_C < P_C \left( T_{PHY} + \frac{S_h + S_l}{R_1} + \text{EIFS} \right).$$

We split the difference contributed by the two extremes  $1/R_L$  (highest rate among colliding frames is  $R_L$ ) and  $1/R_1$  (lowest rate is  $R_1$ ) by taking the mean

$$T_C = P_C \left( T_{PHY} + (S_h + S_l) \left( \frac{a_1}{R_1} + \frac{a_2}{R_2} + \dots + \frac{a_L}{R_L} \right) + \text{EIFS} \right) \quad (22)$$

where  $a_i$  is the ratio that rate  $R_i$  is the slowest among the colliding frames with  $\sum_{k=1}^L a_k = 1$ .

The steady-state probabilities  $\Pi_i$  are crucial to obtaining  $a_i$ . Since  $n_i = \Pi_i N$  in steady-state, the mean attempt rate of stations using rate  $R_i$  is  $\tau_i \Pi_i N$ . The total attempt rate of the system is  $\sum_{i=1}^L \tau_i \Pi_i N$ . Hence the ratio of transmission attempts of stations using  $R_i$  is

$$c_i = \frac{\tau_i \Pi_i N}{\sum_{k=1}^L \tau_k \Pi_k N} = \frac{\tau_i \Pi_i}{\sum_{k=1}^L \tau_k \Pi_k}.$$

Ignoring the contribution of three or more stations colliding simultaneously [5] (their contribution is marginal unless  $N$  is very large), pairwise collisions are given by  $c_i c_i$  (between the same rate  $R_i$ ) and  $2c_i c_j$  for  $i < j$  (between different rates  $R_i$  and  $R_j$ ). Thus

$$a_i = c_i c_i + c_i \left( \sum_{j=i+1}^L c_j \right) + \left( \sum_{j=i+1}^L c_j \right) c_i = c_i^2 + 2c_i \sum_{j=i+1}^L c_j \quad (23)$$

for  $1 \leq i < L$  and  $a_L = c_L^2$ . Substituting into (22), we obtain an estimate of  $T_C$ . In Section IV, we show that the combined ARF-DCF model yields accurate prediction of multi-rate 802.11 WLAN performance.

#### D. Interaction of ARF with RTS/CTS

It has been noted [14], [17] that RTS/CTS (by default inactive in WLAN cards) can be useful in helping ARF distinguish noise from collision, both of which result in frame transmission failure. Since an RTS frame is transmitted at the lowest data rate and its size is small, a failure in RTS frame transmission is likely to stem from collision. On the other hand, unsuccessful data frame transmission following a successful RTS/CTS handshake is likely the result of channel noise. A modified ARF that makes use of this information, assuming RTS/CTS is enabled (there are overhead issues), can help discriminate channel noise from collision. The influence of RTS/CTS on ARF performance is easily captured in our ARF-backoff model by recalculating the slot duration expressions

$$\begin{aligned} T_{S(k)}^{rts} &= T_{RTS} + T_{CTS} + 2SIFS + T_{S(k)}^{bas}, \\ T_{Err(k)}^{rts} &= T_{RTS} + T_{CTS} + 2SIFS + T_{Err(k)}^{bas}, \\ T_C^{rts} &= T_{RTS} + EIFS, \end{aligned}$$

where  $T_{RTS}$  and  $T_{CTS}$  are the slot durations of RTS and CTS frames.

## IV. COMBINED ARF-DCF PERFORMANCE VALIDATION

We evaluate the predictive accuracy of the combined ARF-DCF IEEE 802.11 WLAN model by comparing the analytical results with *ns-2* simulations. We consider both IEEE 802.11b and 802.11g environments. The parameters used in the analyses and simulations are shown in Table I.

#### A. ARF Rate Distribution

Section II-C showed performance validation of the ARF Markov chain when  $p_i$ ,  $i \in \{1, \dots, L\}$ , were given. In this section we show combined ARF-DCF results when the  $p_i$  are determined by the combined ARF-DCF model. Fig. 5 compares predicted steady-state rate distribution  $\Pi_i$  in the combined ARF-DCF

TABLE I  
802.11B/G PARAMETERS USED IN THE PERFORMANCE EVALUATION

Parameter	802.11b	802.11g
aSlotTime ( $\sigma$ )	20 $\mu$ sec	9 $\mu$ sec
SIFS	10 $\mu$ sec	10 $\mu$ sec
DIFS	50 $\mu$ sec	28 $\mu$ sec
PHY header ( $T_{PHY}$ )	192 bits/1Mbps	192 bits/12Mbps
ACK	112 bits/1Mbps + PHY header	112 bits/12Mbps + PHY header
RTS ( $T_{RTS}$ )	160 bits/1Mbps + PHY header	160 bits/6Mbps + PHY header
CTS ( $T_{CTS}$ )	112 bits/1Mbps + PHY header	112 bits/6Mbps + PHY header
LongRetryLimit	4	4
ShortRetryLimit	7	7

IEEE 802.11b model with simulation results. Simulation duration is 1000 seconds. The results show that the combined solution obtained from parameterized coupling of the ARF and DCF chains gives accurate

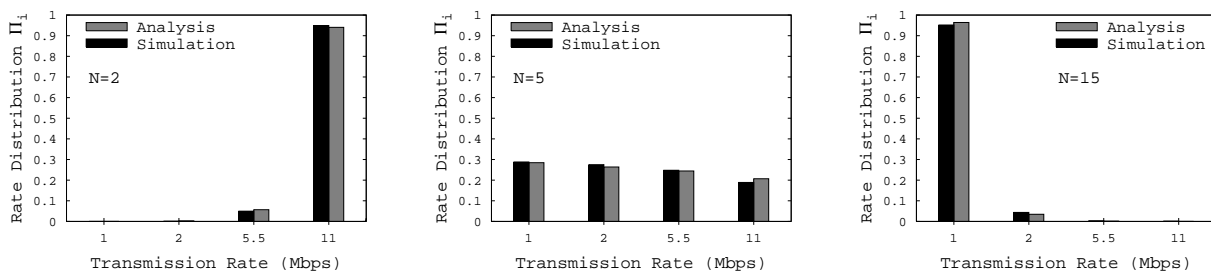


Fig. 5. Rate distribution ( $\Pi_i$ ): Combined ARF-DCF analysis vs. simulation ( $\theta_u=10$ ,  $\theta_d=2$ ) for  $N = 2, 5$ , and 15 in IEEE 802.11b (moderate error).

performance predictions. Fig. 6 shows the corresponding results for IEEE 802.11g which has  $L = 8$  data rates. We find accurate agreement of  $\Pi_i$  between the combined ARF-DCF model and  $ns-2$  simulation results which forms the basis for throughput comparisons under different PHY environments.

### B. Combined ARF-DCF Throughput

Fig. 7 compares combined ARF-DCF throughput predicted by analysis with simulation for 802.11b as the number of contending stations  $N$  is varied. We consider two channel conditions with different bit error rates: (i) moderate noise at which  $\text{BER}_{11\text{Mbps}} = 10^{-6}$  for 802.11b, and (ii) high noise at which  $\text{BER}_{11\text{Mbps}} = 10^{-3}$  for 802.11b (the impact of noise is evaluated in the next section). The resultant FER (i.e.,  $e_1, e_2, \dots, e_L$ ) of each PHY modulation is determined by empirical BER versus SNR curves from Intersil [2]. Under moderate channel noise conditions, we find a *unimodal, bell-shaped curve* whose

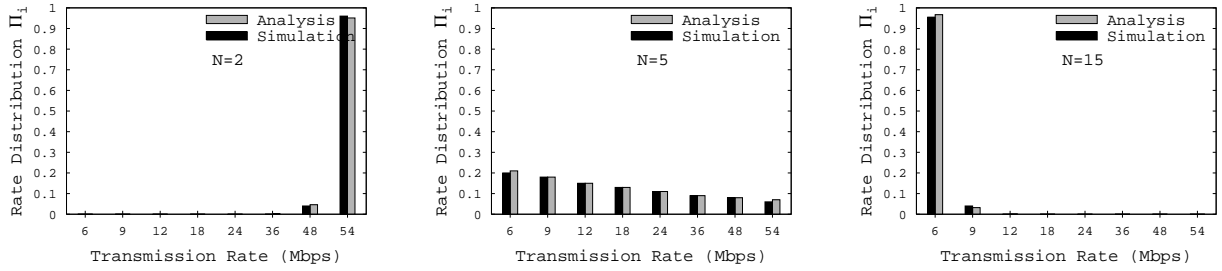


Fig. 6. Rate distribution ( $\Pi_i$ ): Combined ARF-DCF analysis vs. simulation ( $\theta_u=10$ ,  $\theta_d=2$ ) for  $N = 2, 5$ , and 15 in IEEE 802.11g (moderate error).

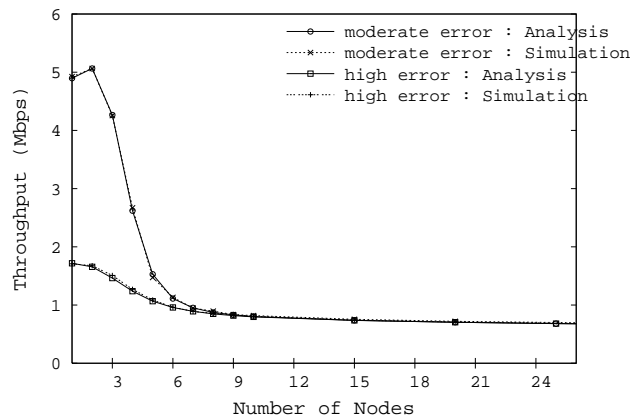


Fig. 7. IEEE 802.11b combined ARF-DCF throughput as a function of contention level: Analysis vs. simulation.

throughput drops precipitously under moderate contention, consistent with empirical performance results from real-world IEEE 802.11b WLANs [9]. The skewness in  $\Pi_i$  caused by ARF's inability to effectively differentiate channel noise from collision translates to a steep decline in throughput. When channel noise is high, the throughput decline due to ARF's missteps is significantly dampened but still present (down to a factor of 2 from a factor of more than 5).

Fig. 8 shows the corresponding results for IEEE 802.11g. The values for moderate and high noise are  $\text{BER}_{54\text{Mbps}} = 10^{-6}$  and  $\text{BER}_{24\text{Mbps}} = 10^{-3}$ . The results show that the combined ARF-DCF model gives accurate quantitative predictions of IEEE 802.11 performance in the presence of cross-layer protocol interactions.

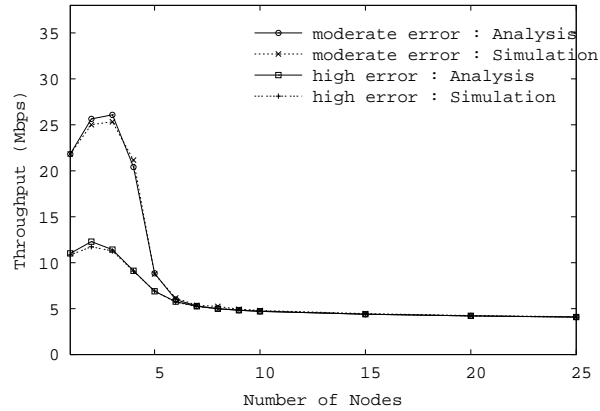


Fig. 8. IEEE 802.11g combined ARF-DCF throughput as a function of contention level: Analysis vs. simulation.

### C. DCF Throughput with RTS/CTS

In this section, we incorporate the impact of RTS/CTS. Figs. 9 show DCF throughput of 802.11b and 802.11g with RTS/CTS under ARF-backoff analysis and *ns-2* simulation. The combined backoff-ARF model predicts that for moderate channel noise RTS/CTS helps improve ARF's frame error vs. collision discrimination capability which mitigates the sharp throughput decline. This comes, however, at the cost

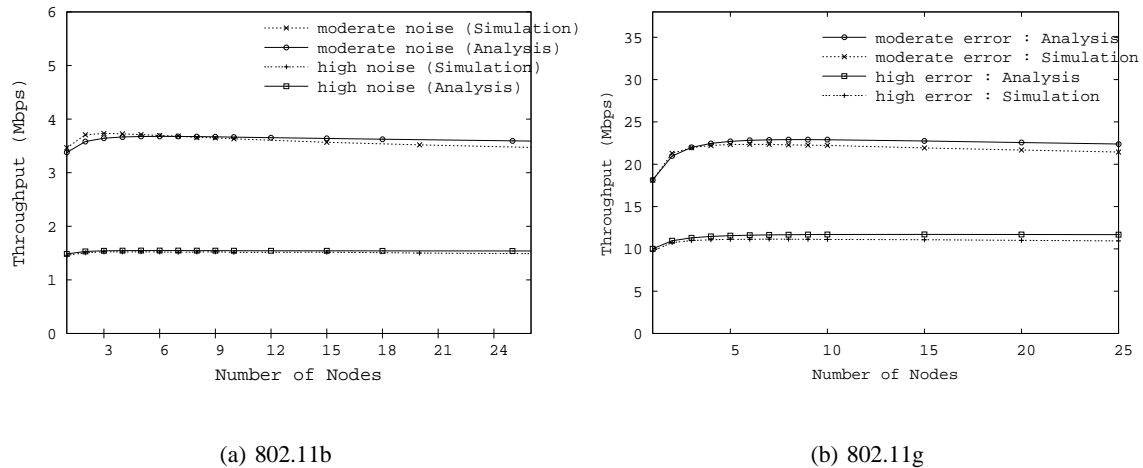


Fig. 9. IEEE 802.11 DCF throughput with RTS/CTS as a function of contention level: Simulation vs. analysis. (a) 802.11b (b) 802.11g

of RTS/CTS overhead which keeps throughput below 4 Mbps. Figs. 9 show that the performance benefit of RTS/CTS is more muted when channel noise is high.

#### D. Effect of Channel Noise

We evaluate predictive accuracy of the combined ARF-DCF model over a wide range of stationary channel noise. Fig. 10 compares throughput from analysis and simulation as a function of SNR with and without RTS/CTS when  $N = 1$  (to remove multiple access contention). The fixed-rate curves for 1, 2, 5.5, and 11 Mbps from physical measurements are shown for reference. We observe that predictive accuracy remains high over a wide range of SNR values.

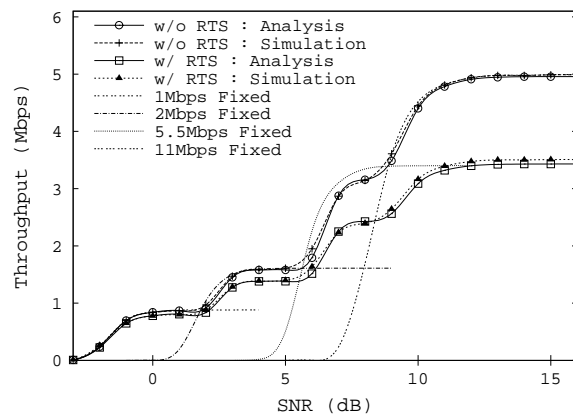


Fig. 10. IEEE 802.11b combined ARF-DCF throughput: Analysis vs. simulation ( $\theta_u = 10$ ,  $\theta_d = 2$ ) with and without RTS/CTS.

#### E. Model-based ARF Calibration

We utilize the accurate predictive power of the combined ARF-backoff IEEE 802.11 model to characterize ARF performance under different channel conditions and calibrate existing ARF implementation based on up/down thresholds  $\theta_u$  and  $\theta_d$ . Fig. 11 shows DCF throughput without RTS/CTS as a function of SNR for IEEE 802.11b. For SNR above 10 dB throughput reaches saturation which shows throughput degradation due to ARF's response to multiple access contention in the low noise regime. At the opposite end when SNR is below 3 dB, channel errors dominate collision and ARF throughput collapses across different  $N$  values. In-between we find two inflection regions (plateaus in the case of small  $N$ ) that correspond to modes of  $\Pi_i$  located at intermediate rates 2 and 5.5 Mbps.

Fig. 12 shows ARF-DCF throughput for different combinations of up/down thresholds at the channel condition of SINR=8dB at which  $\text{BER}_{11\text{Mbps}} = 10^{-3}$  as contention level  $N$  is varied. We observe that the performance of the default values  $\theta_u = 10$  and  $\theta_d = 2$  implemented in WLAN cards drops sharply as the number of contending station  $N$  increases. When asymmetry is injected in the opposite direction,

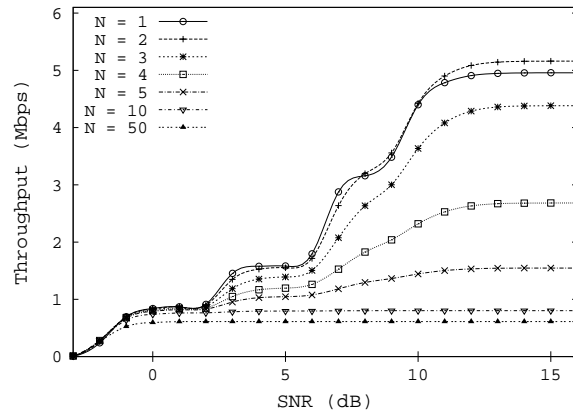


Fig. 11. Basic DCF throughput versus SNR ( $\theta_u=10$ ,  $\theta_d=2$ )

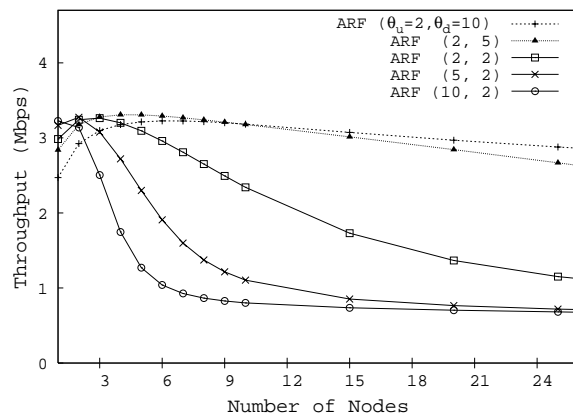


Fig. 12. ARF-DCF throughput for various  $\theta_u$  and  $\theta_d$  combinations.

i.e.,  $\theta_u = 2$  and  $\theta_d = 10$ , throughput significantly improves even at high contention (i.e., large  $N$ ) thanks to its value of large down-threshold which prevents the detrimental rate downshift due to collisions. Note that in fast-fading channels the configuration  $\theta_u = 2$ ,  $\theta_d = 10$  may be more suited since a large down-threshold can be detrimental due to slow responsiveness.

## V. SCALABLE PERFORMANCE OF TCP-OVER-WLAN WITH ARF

### A. Interaction of TCP with ARF and DCF

We showed that the combined ARF-DCF model accurately captures and predicts the dynamics of multi-rate 802.11 WLANs. This includes the ARF performance anomaly [9], [13] which has been a source of confusion. For example, in [26] the throughput decline with increasing  $N$  observed in

empirical WLAN measurements was attributed to congestion stemming from multiple access contention. We also showed that the ARF-DCF model can be easily extended to incorporate the mitigating effect of RTS/CTS, and facilitates ARF calibration and optimization that may aid future system design. Another important component in inter-layer protocol interaction is the influence of TCP. IEEE 802.11 WLANs are predominantly used to access the Internet, and like their wireline brethren [21], the bulk of the workload is TCP-mediated file traffic [25]. In [9] empirical TCP-over-WLAN measurements have shown that TCP has a mitigating influence on ARF resulting in WLAN throughput that outperforms throughput under RTS/CTS and ARF threshold calibration. In this section we incorporate the influence of TCP in cross-layer WLAN analysis to help explain the empirical results.

### B. Markov Chain Analysis of TCP-over-WLAN

We consider an IEEE 802.11 infrastructure WLAN where  $N$  TCP wireless stations access the Internet

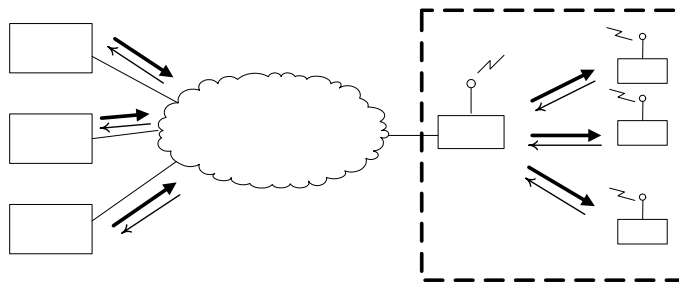


Fig. 13. Wireless/wireline IP network with IEEE 802.11 infrastructure WLAN segment

through a shared AP. We assume a typical client/server environment where each station downloads files transported by TCP, which means that the bulk of TCP data traffic flows downstream—from server through AP to wireless clients—and the bulk of upstream traffic is TCP ACK traffic (see Fig. 13). We ignore differences in wireline bandwidth and delay from AP to servers which can cause TCP unfairness issues on the wireline side. We assume each station uses TCP NewReno without SACK and delayed ACK is disabled. Enabling delayed ACK mainly changes the traffic ratio between AP and wireless stations. We consider steady-state behavior under heavy traffic conditions where all flows are long-lived (i.e., infinite source).

1) *TCP-over-DCF Dynamics*: The AP's role in the 802.11 infrastructure WLAN environment is to forward downstream traffic from wireline servers to wireless stations. A client station's egress buffer is empty until a data frame is received from the AP. This triggers an upstream TCP ACK response which

increases the station's buffer by one data frame and makes it contend for the wireless channel. Since DCF provides equal channel access opportunity to all wireless stations including the AP, the traffic rate (in packet unit) in steady-state contributed by the AP vis-à-vis a wireless station is  $N : 1$ . Also, when the wireline bandwidth to the AP is higher than the effective capacity of the WLAN segment, the AP's egress buffer is under constant backlog [9]. Commodity APs experience maximum sojourn time in the 0.5–1 sec range which depends on the amount of buffer memory. High-end APs (e.g., Enterasys RoamAbout) tend to incur higher queueing delay due to more memory. To analyze TCP-over-WLAN performance, we advance a *station-centric* TCP-over-DCF Markov chain that tracks multiple access contention dynamics from a station's perspective. We first analyze the single-rate environment which focuses on scalable TCP-over-DCF performance. This is followed by the multi-rate case where the mitigating influence of TCP-over-DCF on ARF is incorporated.

2) *Analysis of Single-rate Case:* An important quantity in TCP-over-WLAN dynamics is the *average number of active (i.e., backlogged) stations*,  $N_a$ , whose small value—resulting from the  $N : 1$  traffic ratio—is the primary reason for scalable TCP-over-DCF performance. From a station's perspective, successful reception of a data frame from the AP leads to an increase in its buffer size by one (which may increase the number of active stations by one if the station was in non-backlogged state), and a successful transmission of a TCP ACK frame to the AP leads to a decrease in the buffer size by one (which may decrease the number of active stations by one if the transmitted packet was the last backlogged frame). To characterize the dynamics, we define a station-centric TCP-over-DCF Markov chain  $Q(t)$  over the state-space of backlogged frames awaiting transmission by DCF. Let  $K$  denote a station's buffer size in packet unit. In the wireless Internet access context,  $Q(t) = k$  if there are  $k$  outstanding TCP ACK packets awaiting transmission at client side. Similarly for the AP due to symmetry (albeit for TCP data packets) since there is no distinction between AP and wireless station in DCF when engaging in CSMA competition. Let  $\lambda_{sta}$  and  $\mu_{sta}$  denote the arrival and departure probabilities of a station's egress buffer. Assuming homogeneous clients in station-centric modeling, due to DCF's symmetry the probability that a station receives a TCP packet from the AP in a given slot is

$$\lambda_{sta} = \frac{1}{N} \tau_{ap} (1 - p_{ap}) \quad (24)$$

where  $\tau_{ap}$  is the AP's attempt rate which follows Eq. (18) and  $p_{ap}$  is its frame transmission failure probability. Assuming no packet discard due to the DCF's maximum retry limit, the departure rate  $\mu_{sta}$  is given by

$$\mu_{sta} = \tau_{sta} (1 - p_{sta}) \quad (25)$$

where  $\tau_{sta}$  is the conditional attempt rate of a station when it has a packet to transmit. In an  $M/M/1/K$  birth-death process, the probability of empty buffer is  $\pi_{sta,0} = (1 - \rho)/(1 - \rho^{K+1})$  where  $\rho = \lambda_{sta}/\mu_{sta}$ . When buffer size  $K$  is large ( $K \rightarrow \infty$ ), we have

$$\pi_{sta,0} = \left(1 - \frac{\lambda_{sta}}{\mu_{sta}}\right) = 1 - \frac{\tau_{ap}(1 - p_{ap})}{N\tau_{sta}(1 - p_{sta})}. \quad (26)$$

Under the constant backlog assumption at the AP (i.e.  $\pi_{ap,0} = 0$ ) stemming from the  $N : 1$  AP-to-wireless station traffic ratio and the AP's wireline/wireless bandwidth mismatch, the conditional transmission failure probabilities are given by

$$p_{ap} = 1 - (1 - e_{ap}) \sum_{n=0}^N P\{N_a = n\}(1 - \tau_{sta})^n,$$

$$p_{sta} = 1 - (1 - e_{sta})(1 - \tau_{ap}) \sum_{n=0}^{N-1} P\{N_a = n\}(1 - \tau_{sta})^n,$$

where  $e_{ap}$  and  $e_{sta}$  are the AP's and station's frame error rates (FERs) due to channel errors, and  $P\{N_a = n\}$  is the probability that the number of active stations is  $n$ . Since  $P\{N_a = n\} = \binom{N}{n} (1 - \pi_{sta,0})^n (\pi_{sta,0})^{N-n}$ , we have

$$p_{ap} = 1 - (1 - e_{ap}) \left\{1 - (1 - \pi_{sta,0})\tau_{sta}\right\}^N,$$

$$p_{sta} = 1 - (1 - e_{sta})(1 - \tau_{ap}) \left\{1 - (1 - \pi_{sta,0})\tau_{sta}\right\}^{N-1}. \quad (27)$$

Eqs. (26)–(27) comprise four equations in four unknowns  $\tau_{ap}$ ,  $\tau_{ap}$ ,  $\tau_{sta}$ , and  $\tau_{sta}$ , which can be solved using fixed-point methods. The active station count, including the AP, in equilibrium is given by

$$E[N_{active}] = E[N_a] + E[N_{ap}] = N(1 - \pi_{sta,0}) + (1 - \pi_{ap,0}). \quad (28)$$

3) *Analysis of Multi-rate Case:* ARF enters into the picture through  $\Pi_{g,i}$ ,  $g \in \{sta, ap\}$ ,  $i \in \{1, \dots, L\}$ , which effects the average transmission rate

$$\bar{\tau}_g = \sum_{i=1}^L \Pi_{g,i} \tau_{g,i}, \quad g \in \{sta, ap\}.$$

Since the transmission failure probabilities  $p_{g,i}$  are given by (see Eq. (20) in Section III-B)

$$p_{ap,i} = 1 - \left\{1 - (1 - \pi_{sta,0})\bar{\tau}_{sta}\right\}^N (1 - e_{ap,i}),$$

$$p_{sta,i} = 1 - (1 - \bar{\tau}_{ap}) \left\{1 - (1 - \pi_{sta,0})\bar{\tau}_{sta}\right\}^{N-1} (1 - e_{sta,i}), \quad (29)$$

we use modular coupling from ARF-DCF analysis to solve the fixed-point problem with increased dimension introduced by  $\Pi_{g,i}$ . Throughput calculation for TCP-over-DCF with ARF follows the steps described in Section III-C, accounting for differences in TCP data and ACK frame sizes.

### C. TCP-over-WLAN Performance Validation

1) *Scalable TCP-over-DCF Throughput*: Fig. 14 shows TCP-over-DCF throughput (both with and without RTS/CTS) as the number of contending wireless stations  $N$  is increased from 1 to 25. The results from TCP-over-DCF Markov chain analysis predict throughput obtained from *ns-2* simulation. Even with 25 contending stations, there is hardly any throughput decline. Its key reason lies in the

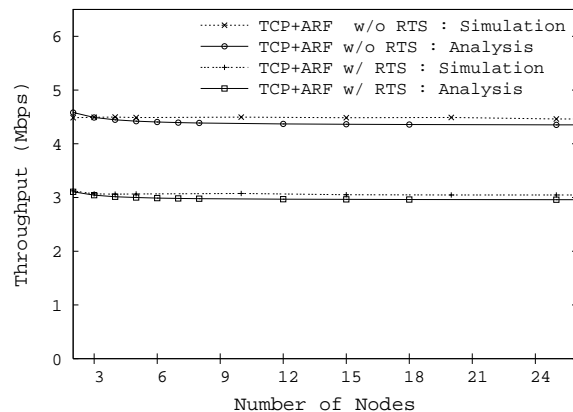


Fig. 14. Scalable TCP-over-DCF with and without RTS/CTS in the presence of ARF as a function of number of contending stations  $N$ .

$O(1/N)$ -factor difference between  $\lambda_{sta}$  and  $\mu_{sta}$  in a station’s TCP-over-DCF birth-death chain which imparts a strong negative drift for large  $N$  that inhibits the growth of a station’s backlog queue in the presence of heavy multiple access contention. The results are consistent with the empirical results in [9].

From a “station versus AP perspective,” the  $O(1/N)$ -factor difference between  $\tau_{ap}$  and  $\tau_{sta}(1 - \pi_{sta,0})$  captures the fact that an AP—because it competes equally with stations under DCF—is unlikely to win a multiple access competition when  $N$  is large. The larger the number of backlogged stations, the smaller the probability that the AP will succeed in transmitting a data packet to a station which would increase the backlog queue of an already backlogged station or increase the number of backlogged stations. This effect can be seen in Table II which shows the average number of backlogged stations  $N_{active}$  as a function  $N$ . The results from TCP-over-DCF analysis show that the average number of backlogged stations in equilibrium is a little over 2 (and well below 3) even for large  $N$ . This implies that *the effective multiple access contention* experienced by TCP-over-DCF remains invariant at 2–3 stations resulting in low collision and high system throughput.

2) *TCP’s Mitigating Effect on ARF*: Fig. 14 also shows the mitigating effect of TCP-over-DCF on ARF which, unlike the bell-shaped ARF-DCF throughput curves in Figs. 7 and 12 without TCP, remain

TABLE II  
BACKLOGGED STATIONS  $N_{active}$  AS A FUNCTION OF CONTENDING STATIONS  $N$

$N$	2	5	10	20	50	100
$\Pr\{\text{buffer size} > 0\} (=1 - \pi_{sta,0})$	0.53	0.22	0.11	0.06	0.02	0.01
Analysis: $N_{active}$	2.07	2.11	2.12	2.13	2.14	2.14
Simulation: $N_{active}$	2.14	2.16	2.17	2.20	2.23	2.26

flat as contention level  $N$  is increased. The main reason for ARF not getting miscued by collision is the low collision rate afforded by scalable TCP-over-DCF throughput which renders consecutive collision unlikely. When they occasionally occur, recovery is fast. This allows ARF to focus on frame errors stemming from channel noise in accordance with its intended design.

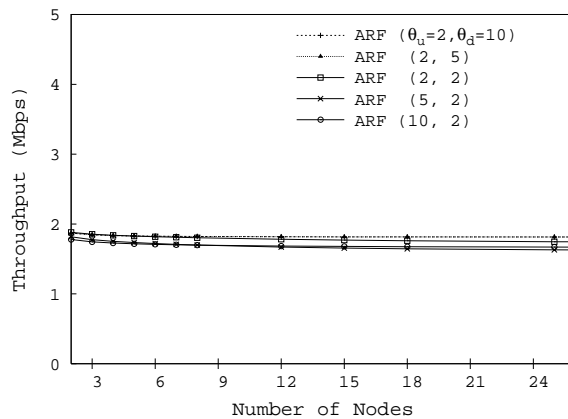


Fig. 15. TCP-over-WLAN throughput in the presence of ARF for various  $\theta_u$  and  $\theta_d$  combinations.

We utilize our model to see the effect of ARF's thresholds on the performance of TCP-over-DCF. Fig. 15 shows the throughput of TCP-over-DCF with ARF for different combinations of up/down thresholds at the channel condition of high noise at which  $\text{BER}_{11\text{Mbps}} = 10^{-3}$ . It shows that the mitigating influence of TCP is insensitive to details in the underlying ARF parameters, unlike the results in Fig. 12.

## VI. CONCLUSION

In this paper, we have advanced station-centric Markov chain models of protocol interaction between ARF, DCF, and TCP in multi-rate IEEE 802.11 WLANs. We have shown that the performance analyses

accurately predict cross-layer WLAN behavior, capturing subtle and complex system traits such as bell-shaped throughput curve under ARF-DCF and scalable throughput of TCP-over-WLAN. This is achieved through modular coupling which finds parameterized solutions to subsystems that are joined to form a globally consistent solution. We show that modular coupling facilitates tractable analysis by curbing the state-space explosion of direct analysis without sacrificing accuracy. The station-centric performance analysis spanning transport, MAC, and PHY layers may be viewed as a multi-protocol extension of Bianchi's IEEE 802.11 DCF model, which demonstrates the versatility and efficacy of station-centric Markov chain modeling for capturing cross-layer WLAN dynamics. A number of issues remain for future work. They include finding a solution to an optimal ARF design problem using a Markov decision process approach enabled by the ARF-DCF chain, analysis of ARF under fading channels that exhibit correlated errors, and establishing rigorous foundations for modular coupling as an approximation technique in station-centric cross-layer analysis.

#### REFERENCES

- [1] IEEE, Part 11: Wireless LAN Medium Access Control (MAC) and Physical Layer (PHY) Specifications. IEEE Std 802.11-1999, 1999.
- [2] Intersil, "HFA3861B; Direct Sequence Spread Spectrum Baseband Processor," 2000.
- [3] <http://www.enterasys.com/>, online link.
- [4] H. Balakrishnan, V. Padmanabhan, S. Seshan, and R. Katz, "A comparison of mechanisms for improving TCP performance over wireless links," *IEEE/ACM Trans. Networking*, 5(6):756–769, 1997.
- [5] G. Bianchi, "Performance Analysis of the IEEE 802.11 Distributed Coordinated Function," *IEEE J. Selected Areas in Commun.*, vol. 18, no. 3, pp. 535-547, 2000.
- [6] J. Bicket, "Bit-rate selection in wireless networks," Masters thesis, Massachusetts Institute of Technology, 2005.
- [7] P. Chevillat, J. Jelitto, A. Barreto, and H. Truong, "A Dynamic Link Adaptation Algorithm for IEEE 802.11a Wireless LANs," in *Proc. IEEE ICC03*, pp. 1141-1145, 2003.
- [8] J. Choi, K. Park, and C. Kim, "Cross-Layer Analysis of Rate Adaptation, DCF and TCP in Multi-Rate WLANs," in *Proc. IEEE INFOCOM07*, pp. 1055-1063, 2007.
- [9] S. Choi, K. Park, and C. Kim, "On the Performance Characteristics of WLANs: Revisited," in *Proc. ACM SIGMETRICS'05*, pp. 97-108, 2005.
- [10] Z. Hadzi-Velkov and B. Spasenovski, "An analysis of CSMA/CA protocol with capture in Wireless LANs," in *Proc. IEEE WCNC'03*, vol.2 pp. 16-20, 2003.
- [11] W. Haitao, P. Yong, L. Keping, C. Shiduan, and M. Jian, "Performance of reliable transport protocol over IEEE 802.11 wireless LAN: Analysis and enhancement," in *Proc. IEEE INFOCOM '02*, pages 599–607, 2002.
- [12] I. Hatatcherev, K. Langendoen, R. Lagendijk, H. Sips, "Hybrid rate control for IEEE 802.11," in *Proc. ACM MobiWac'04*, pp.10-18, 2004.
- [13] M. Heusse, F. Rousseu, G. Berger-Sabbatel, and A. Duda, "Performance Anomaly of 802.11b," in *Proc. IEEE INFOCOM'03*, pp. 836-843, 2003.

- [14] C. Hoffmann, M. Manshaei, T. Turletti, "CLARA: Closed-Loop Adaptive Rate Allocation for IEEE 802.11 WirelessLANs," in *Proc. IEEE WIRELESSCOM'05*, 2005.
- [15] V. Joel. "Exploding the myth of WLAN performance," Telephony Online, 2004.
- [16] A. Kamerman and L. Monteban, "WaveLAN 2: A High-performance Wireless LAN for the Unlicensed Band," *Bell Labs Tech. Journal*, 1997.
- [17] J. Kim, S. Kim, S. Choi, and D. Qiao, "CARA: Collision-Aware Rate Adaptation for IEEE 802.11 WLANs," in *Proc. IEEE INFOCOM'06*, 2006.
- [18] M. Lacage, M. H. Manshaei, T. Turletti, "IEEE 802.11 rate adaptation: a practical approach," in *Proc. ACM MSWiM'04*, pp. 126-134, 2004.
- [19] J. Padhye, V. Firoiu, D. Towsley, and J. Kurose, "Modeling TCP throughput: A simple model and its empirical validation," in *Proc. ACM SIGCOMM '98*, pp. 303-314, 1998.
- [20] Q. Pang, Leung, V. Liew, S. Liew, "A rate adaptation algorithm for IEEE 802.11 WLANs based on MAC-layer loss differentiation," in *Proc. IEEE Broadband Networks'05*, pp. 709-717, 2005.
- [21] K. Park and W. Willinger, "Self-similar network traffic: An overview," in K. Park and W. Willinger, editors, *Self-Similar Network Traffic and Performance Evaluation*. Wiley-Interscience, 2000.
- [22] K. Pentikousis, "TCP in wired-cum-wireless environments," *IEEE Communications Surveys*, Fourth Quarter(7):2-14, 2000.
- [23] D. Qiao and S. Choi, "Fast-Responsive Link Adaptation for IEEE 802.11 WLANs," in *Proc. IEEE ICC'05*, pp. 3583-3588, 2005.
- [24] G. Sharma, A. Ganesh and P. Key, "Performance analysis of Contention Based Medium Access Control Protocols," in *Proc. IEEE INFOCOM'06*.
- [25] D. Tang, M. Baker, "Analysis of a Local-Area Wireless Network," in *Proc. ACM MobiCom'00*, pp. 1-10, 2000.
- [26] A. Vasani and U. Shankar. "An empirical characterization of instantaneous throughput in 802.11b WLANs," *Technical Report CS-TR-4389, UMIACS-TR-2002-69, Department of Computer Science and UMIACS, University of Maryland College Park*, 2002.
- [27] H. Y. Wong, H. Yang, S. Lu, and V. Bharghavan, "Robust Rate Adaptation for 802.11 Wireless Networks," in *Proc. ACM Mobicom06*, pp. 146-157, 2006
- [28] H. Wu, Y. Peng, K. Long and J. Ma, "Performance of Reliable Transport Protocol over IEEE 802.11 Wireless LAN: Analysis and Enhancement," in *Proc. IEEE INFOCOM'02*, vol.2, pp. 599-607, 2005.
- [29] Y. Xiao, "An Analysis for Differentiated Services in IEEE 802.11 and IEEE 802.11e Wireless LANs," in *Proc. ICDCS'04*, 2004.
- [30] G. Xylomenos and G. Polyzos, "TCP and UDP performance over a wireless LAN," in *Proc. IEEE INFOCOM '99*, pp. 439-446, 1999.
- [31] G. Xylomenos, G. Polyzos, P. Mähönen, and M. Saaranen, "TCP performance issues over wireless links," *IEEE Communications Magazine*, vol. 39(4), pp. 52-58, 2001.
- [32] D. Yang, T. Lee, K. Jang, J. Chang and S. Choi, "Performance Enhancement of Multi-Rate IEEE 802.11 WLANs with Geographically-Scattered Stations," *IEEE Trans. Mobile Computing*, vol. 5, no. 7, pp. 906-919, 2006.
- [33] E. Ziouva and T. Antonakopoulos, "CSMA/CA performance under high traffic conditions: throughput and delay analysis," *Computer Communications*, vol. 25, pp.313-321, 2002.